Molecular Cell
Article

The Evolutionarily Conserved Core Design of the Catalytic Activation Step of the Yeast Spliceosome

Patrizia Fabrizio,[1] Julia Dannenberg,[1] Prakash Dube,[2] Berthold Kastner,[1] Holger Stark,[2,4] Henning Urlaub,[3] and Reinhard Lührmann[1,*]
[1]Department of Cellular Biochemistry
[2]3D Electron Cryomicroscopy Group
[3]Bioanalytical Mass Spectrometry Group
Max Planck Institute for Biophysical Chemistry, Am Fassberg 11, D-37077 Göttingen, Germany
[4]Göttingen Center of Molecular Biology, University of Göttingen, Justus-von-Liebig Weg 11, D-37077 Göttingen, Germany
*Correspondence: reinhard.luehrmann@mpi-bpc.mpg.de
DOI 10.1016/j.molcel.2009.09.040

SUMMARY

Metazoan spliceosomes exhibit an elaborate protein composition required for canonical and alternative splicing. Thus, the minimal set of proteins essential for activation and catalysis remains elusive. We therefore purified in vitro assembled, precatalytic spliceosomal complex B, activated B^{act}, and step 1 complex C from the simple eukaryote *Saccharomyces cerevisiae*. Mass spectrometry revealed that yeast spliceosomes contain fewer proteins than metazoans and that each functional stage is very homogeneous. Dramatic compositional changes convert B to B^{act}, which is composed of ~40 evolutionarily conserved proteins that organize the catalytic core. Additional remodeling occurs concomitant with step 1, during which nine proteins are recruited to form complex C. The moderate number of proteins recruited to complex C will allow investigations of the chemical reactions in a fully defined system. Electron microscopy reveals high-quality images of yeast spliceosomes at defined functional stages, indicating that they are well-suited for three-dimensional structure analyses.

INTRODUCTION

Splicing of premessenger RNA (pre-mRNA) is catalyzed by the spliceosome, a large ribonucleoprotein (RNP) comprising several small nuclear (sn)RNPs and numerous proteins (reviewed by Brow, 2002; Wahl et al., 2009). Pre-mRNA splicing takes place in all eukaryotic organisms investigated to date—from metazoans to yeast. The existence of alternative patterns of splicing for a given gene is a major factor in enhancing the relative diversity of eukaryotic proteomes compared with their corresponding genomes.

The spliceosome assembles on its pre-mRNA substrate in an ordered process that begins with recognition of the 5′ end of the intron (5′ splice site [5′ss]) by the U1 snRNP. Thereafter, the U2 snRNP binds to the pre-mRNA's branch site, forming complex A. Complex A then binds the preformed U4/U6·U5 tri-snRNP to form complex B, which contains a full set of UsnRNAs in a precatalytic state. Complex B is then activated for catalysis by a major rearrangement of its RNA network and its overall structure; this remodeling includes dissociation of the U1 and U4 snRNAs and the formation of the activated spliceosome (henceforth named B^{act}). In the catalytically activated complex (termed B*), step 1 of splicing takes place: the adenosine at the branch site attacks the 5′ss, generating a cleaved 5′ exon and intron 3′ exon intermediate. The resulting complex C then catalyzes step 2 of splicing, in which the intron is cleaved at the 3′ splice site (3′ss) with concomitant ligation of the 5′ and 3′ exons.

A complex RNA network involving the snRNAs and pre-mRNA plays a central part in determining the spliceosome's overall structure and in juxtaposing the reaction partners of the pre-mRNA. RNA structures containing U2 and U6 snRNA play a crucial role in the catalytic core of the spliceosome, including direct participation in chemical catalysis (Nilsen, 1998). However, spliceosomal proteins are not mere passive building blocks in this process; proteins carry out essential recognition and catalytic functions during the assembly of the spliceosome and the catalytic reactions (Abelson, 2008; Pyle, 2008), including conformational changes and the selection of intron substrates during "alternative splicing" (Caceres and Kornblihtt, 2002).

The spliceosome is a protein-rich molecular machine. Human spliceosomes contain more than 50 proteins associated with snRNPs and more than 100 non-snRNP proteins as revealed by mass spectrometric studies (Wahl et al., 2009 and references therein). Such studies showed that the spliceosome's protein complement varies substantially from one stage of the splicing cycle to another. For example, a dramatic change in protein composition occurs at the transition from complex B to C alongside the change in RNA composition referred to above (Bessonov et al., 2008).

The isolation of a yeast complex consisting of all five spliceosomal snRNPs (termed the penta-snRNP; Stevens et al., 2002)

led to the hypothesis that the spliceosome can also exist in a preassembled form such that all of the snRNPs could interact concomitantly with the pre-mRNA. However, all of the major remodeling events described above, as well as changes in the composition of the spliceosome, would still be required to generate its catalytically active RNP structure (Brow, 2002).

The pathway of spliceosome assembly and the main features of its catalytic chemistry appear to be conserved between metazoans and yeast. The study of the extent of conservation is not only relevant for tracing evolutionary relationships, but it can also lead to conclusions about the mechanisms of conformational changes, such as those resulting in spliceosome activation or catalysis. Thus, we set out to study isolated spliceosomal complexes from the lower eukaryote *Saccharomyces cerevisiae*, as it was already known to possess a basic (constitutive) spliceosomal machinery similar to that of primates.

A summary of the yeast assembly pathway is shown in Figure 1A (Cheng and Abelson, 1987); for clarity, the yeast complexes are named throughout the paper according to the human nomenclature. First, the yeast system provides elegant methods to stall complexes at defined functional stages (Figure 1B) (Cheng, 1994; Rymond and Rosbash, 1985; Vijayraghavan et al., 1986). Second, yeast is accessible to genetic manipulation and to mutation studies. Third, problems concerning stoichiometry in the human spliceosome, notably with the so-called SR proteins (Hertel and Graveley, 2005), are less likely to arise in the yeast spliceosome, as these proteins are nearly absent (Kress et al., 2008). Finally, alternative splicing (i.e., usage of alternative splice sites) is extremely rare in yeast. This may be expected to simplify functional assignment in the yeast spliceosome and, by comparison, potentially in higher organisms as well. In the human spliceosome, the transition from complex B to C involves the association or dissociation of at least 50 proteins (Bessonov et al., 2008). In yeast, this number likely will be restricted to a minimal set of essential proteins. The expected less-complex protein composition of yeast spliceosomes will also provide a significant advantage for three-dimensional (3D) structure analyses.

The use of yeast as a model for splicing requires the analysis of the yeast spliceosome at all stages of function. Each new round of splicing generates a catalytic center de novo during the transitions from complex B to B^{act} to B^* and to the product of step 1 of splicing, complex C. Here, we focused on the B, activated B^{act}, and C complexes. Each stalled complex was isolated by centrifugation and affinity selection (Deckert et al., 2006; Jurica and Moore, 2002), their proteomes determined by mass spectrometry (MS), and their structures examined by electron microscopy (EM). Our data provide an inventory of the evolutionarily conserved splicing factors that are stably associated during three ''snapshots'' of *S. cerevisiae* spliceosome assembly, activation, and catalysis and offer insights into the window of function of the proteins exchanged during the transition from one stage to the next. EM analyses show the first images of yeast spliceosomes at different stages of function. These are at an unprecedented quality level and should be well suited for 3D structure analyses, based on criteria such as their structural integrity and homogeneity.

RESULTS

Stalling the Yeast Spliceosome at Defined Stages

To isolate preparative amounts of biochemically homogenous complex B, B^{act}, and C, we used an actin pre-mRNA and modifications thereof. For MS2 affinity purification, we fused three MS2-binding sites to the 5′ end of the various pre-mRNA constructs. We term the resulting pre-mRNA ''M3-Act.''

Previous studies showed that truncation/modification of the actin pre-mRNA and adjustment of the ATP concentration in the splicing reaction can lead to stalling of the spliceosomal cycle (Figure 1B) (Cheng, 1994; Rymond and Rosbash, 1985; Vijayraghavan et al., 1986). The intron in the actin pre-mRNA contains the yeast consensus branch site sequence UACUAAC. M3-ActΔ6 and M3-ActΔ31 are truncated 6 and 31 bases, respectively, after this sequence and thus lack the 3′ss and the 3′ exon. The variant M3-ActACAC contains a mutation at the 3′ss (AGAG to ACAC), which is followed by an unmutated but shortened 3′ exon. The presence of three MS2-binding sites at the 5′ end did not inhibit the splicing of wild-type actin pre-mRNA (see below). The abilities of each of the four pre-mRNAs to undergo spliceosome formation and splicing are shown in Figure 2. Spliceosome assembly was detected by electrophoresis on ''native'' gels (Figures 2A and 2C) and splicing, per se, on denaturing gels (Figures 2B and 2D). The inclusion of only 0.05 mM ATP in the splicing reaction led to stalling at the stage of complex B, both for M3-Act and M3-ActΔ6 (Figures 2A and 2B, lanes 5–8 and 13–16), as described for wild-type actin pre-mRNA (Tarn et al., 1993). Raising the ATP concentration to 2.0 mM allowed splicing to proceed to completion for M3-Act (lanes 1–4), whereas for M3-ActΔ6, B complex was converted to the activated B^{act} complex (Figure 2A, lanes 9–12), without any detectable splicing intermediates or spliced mRNA (Figure 2B, lanes 9–12).

Under the same conditions, the truncated M3-ActΔ31 pre-mRNA behaved differently than M3-ActΔ6 (Figures 2A and 2B, lanes 17–20); here, spliceosome assembly proceeded to complex C, which was not formed with M3-ActΔ6 (Figures 2A and 2B, lanes 9–12) and was formed with full-length pre-mRNA only at later incubation times (Figures 2A and 2B, lane 4) (Cheng and Abelson, 1987). The appearance of the cleaved 5′ exon and intron 3′ exon intermediates, but no products (Figure 2B), confirmed the identity of the stalled complex as C. The behavior of the M3-ActACAC pre-mRNA (Figures 2C and 2D) was qualitatively similar to that of M3-ActΔ31, but as the intensities of the bands on the gels show, the yield of C complex was higher with M3-ActACAC. The amount of earlier complexes containing unspliced pre-mRNA was further reduced by adding a DNA oligonucleotide complementary to nucleotides +13 to +24 downstream of the 5′ss and additional incubation for 20 min. This oligonucleotide directs the excision of the 5′ exon by RNaseH (endogenous in the extract), but only in the unspliced form and not after the pre-mRNA has undergone step 1 of splicing (Figure S2 available online).

Purification of Yeast Spliceosomes

For the preparative isolation of B, B^{act}, and C complexes, the various [^{32}P]-labeled M3-Act substrates described above were

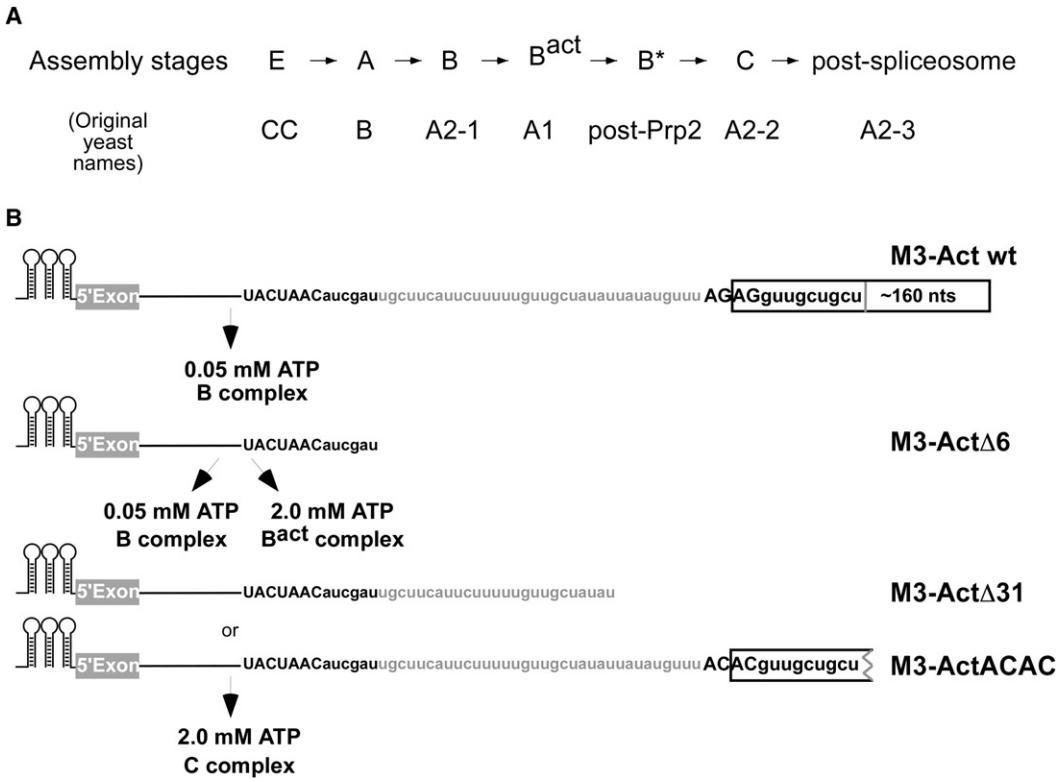

Figure 1. Conditions Used for the Isolation of Yeast Spliceosomes

(A) Spliceosomal complexes are named according to the standard human nomenclature and correspond to the yeast complexes shown (Cheng and Abelson, 1987; Kim and Lin, 1996).

(B) Complex B was assembled on actin WT (Figure S1) or a truncated actin substrate retaining six nucleotides downstream of the branch site UAUAAC sequence (M3-ActΔ6) and was stalled by limiting the ATP concentration in the splicing reaction (Tarn et al., 1993). Complex B^{act} was stalled by using M3-ActΔ6 but increasing ATP to 2.0 mM (Cheng, 1994). Complex C was stalled by using substrates with a missing or mutated 3′ss (M3-ActΔ31 and M3-ActACAC, respectively) (Rymond and Rosbash, 1985; Vijayraghavan et al., 1986).

first incubated with MS2-MBP fusion protein and then subjected to splicing conditions at 23°C for 50–60 min. Subsequently, they were centrifuged in a glycerol gradient to separate B, B^{act}, or C from the majority of other spliceosomal complexes (such as complex A) and from excess MS2-MBP fusion protein. The distribution of spliceosomal complexes in the gradient was determined by measuring the amount of radiolabeled RNA in each fraction, and the peak fractions in the 40S–45S region of the gradient (containing the bulk of B, B^{act}, or C) (data not shown) were pooled and applied to amylose beads, to which the spliceosomal complexes were bound selectively through their MBP. After thorough washing, spliceosomal complexes were eluted under native conditions with excess maltose and were subsequently fractionated on a second glycerol gradient. Their distribution in the gradient was determined, and their RNA and protein contents were subsequently analyzed by denaturing PAGE.

Complex B assembled on M3-ActΔ6 pre-mRNA was prepared as above by performing splicing with 0.05 mM ATP. It exhibited a sedimentation coefficient of ~40S (Figure 3A) and contained nearly equimolar amounts of M3-ActΔ6 pre-mRNA and U2, U4, U5, and U6 snRNAs, whereas U1 was slightly underrepresented (Figure 3B, silver staining). The autoradiography also shows that no splicing intermediates were detected. The preparation therefore contained precatalytic B complex of high homogeneity. The distribution of radioactivity in the glycerol gradient showed, in addition to the main peak at 40S, a second peak of ~20–25S. RNA analysis of this peak revealed the presence of unspliced pre-mRNA and also degradation products of the snRNAs (data not shown). These fractions were therefore not analyzed further. Similar second peaks were also obtained with the other two complexes (Figures S3 and S4).

Complex B^{act} was prepared using M3-ActΔ6 but with 2.0 mM ATP in the splicing reaction. It exhibited a slightly higher S value (~45S) than did complex B (Figure S3A). Nearly stoichiometric amounts of uncleaved pre-mRNA and U2, U5, and U6 snRNAs were detected in these complexes after silver staining and northern blotting, whereas U1 and U4 snRNAs were essentially absent from the B^{act} complex peak (Figure S3B). This indicates that the predominant complex isolated was indeed the activated B^{act} and not the precatalytic B complex. Thus, B^{act} is activated because it has lost U1 and U4, but its protein composition indicates that it is not yet catalytically active (see below).

Complex C was assembled on either M3-ActΔ31 or M3-ActACAC pre-mRNA. This was done to determine whether

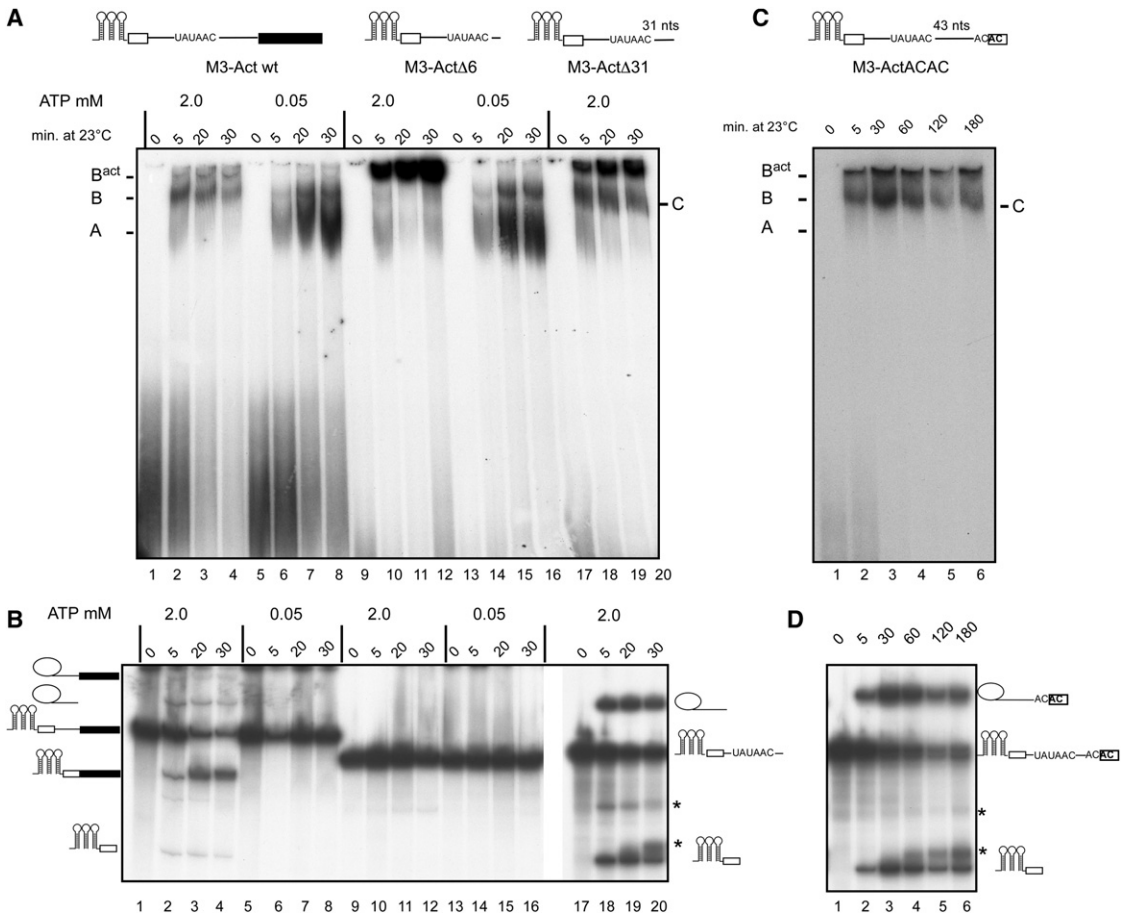

Figure 2. Kinetics of Splicing and Splicing Complex Formation

(A and B) (A) Kinetics of in vitro splicing complex formation and (B) splicing. In lanes 1–8 of both panels, M3-Act WT is used; in lanes 9–16, M3-ActΔ6; in lanes 17–20, M3ActΔ31.

(C and D) (C) Kinetics of in vitro splicing complex formation and (D) splicing using the 3′ss mutated RNA substrate M3-ActACAC. Splicing was performed at 2.0 mM ATP in yeast whole-cell extract for 0–180 min.

In (A) and (C), splicing complexes were analyzed on nondenaturing gels. In (B) and (D), RNA was analyzed by denaturing PAGE. The positions of the complexes, pre-mRNA, and splicing intermediates are indicated on the right and left. (Asterisks) Unknown pre-mRNA-derived bands.

additional factors are recruited to M3-ActACAC as compared to the shorter M3-ActΔ31 pre-mRNA. DNA oligo-directed RNaseH cleavage was subsequently performed to remove earlier splicing complexes. After affinity purification (irrespective of which pre-mRNA was used), complex C exhibited an S value of ~40 and contained similar amounts of U2, U5, and U6 snRNAs, excised 5′ exon, and intron 3′ exon. Less than 5%–10% of unspliced pre-mRNA remained in purified C complex after oligo-directed RNaseH digestion (Figures S4A, S4B, S4C, and S2).

Protein Composition of Purified Yeast Spliceosomes

Proteins isolated from purified complexes were separated by PAGE and visualized by staining with Coomassie or silver. Proteins were subsequently identified by liquid chromatography-coupled tandem mass spectrometry (LC-MS/MS) and scored by the absolute number of peptides found in each preparation The protein composition of each complex was determined in at least two independent experiments and is summarized in Table 1. Note that the molar amounts of individual spliceosomal complexes used for MS differ in independent experiments. The vast majority of proteins were detected reproducibly (i.e., in two out of two preparations). Only a few were found only once, suggesting either that they are loosely associated with spliceosomal complexes and lost during purification or that they may be contaminants.

The purified B complex contained ~60 proteins. These included all known U1- and U2-specific snRNP proteins. Of the U5-specific proteins, Prp8, Brr2, Snu114, Prp6, and Dib1 were present, but not Lin1, which only associates with free U5 particles and not with the U4/U6.U5 tri-snRNP that is integrated into complex B. Furthermore, all U4/U6-specific proteins and the tri-snRNP-specific proteins Snu66, Spp381, Prp38, and Snu23 were detected (Gottschalk et al., 1999; Stevens and Abelson, 1999). Sad1 and the RNA helicase Prp28 were not found in any of the B complex preparations (nor in B^{act} or C preparations). The absence of both proteins was expected, as both

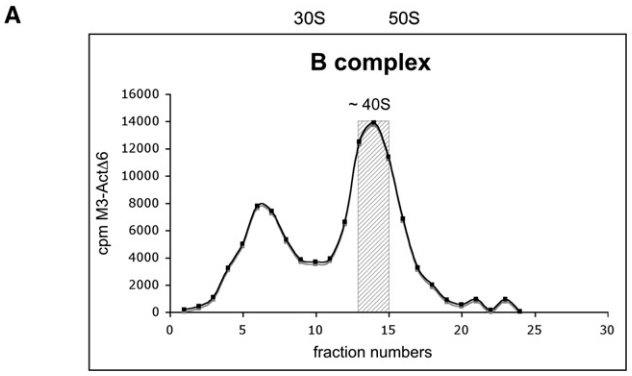

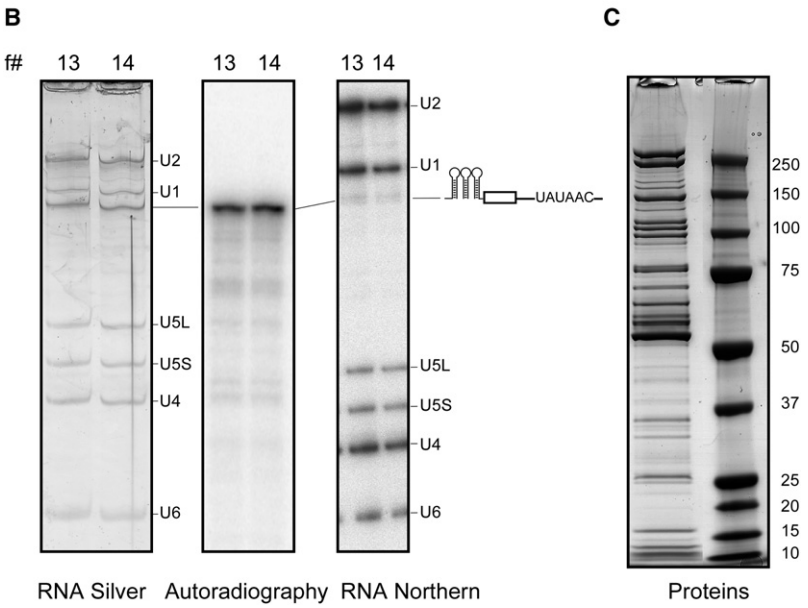

Figure 3. Characterization of Purified B Complex

(A) Profile of purified B complex (specific activity of 100 cpm/fmol) separated on a glycerol gradient. The radioactivity contained in each gradient fraction was determined by Cherenkov counting. Sedimentation coefficients were determined by analyzing the UV absorbance of a reference gradient containing prokaryotic ribosomal subunits.

(B) RNA from gradient fractions 13–14 was recovered, separated by denaturing PAGE, and visualized by silver staining, autoradiography, and northern analysis. RNA identities are indicated on the right.

(C) Proteins were separated by SDS-PAGE and stained with Coomassie.

are associated with only a fraction of yeast tri-snRNP at very low salt (50–70 mM KCl) (P.F. and R.L., unpublished data and Small et al., 2006). The fact that U1 is slightly underrepresented may be expected for a B complex stalled at a stage after Prp28 has acted and indicates a minor destabilization of the U1 snRNP.

All three proteins of the retention and splicing (RES) complex were detected in complex B. This is consistent with previous experiments, indicating that it associates with the yeast spliceosome prior to step 1 (Dziembowski et al., 2004). All eight proteins of the NTC (Prp19) complex were also found in B with significant numbers of peptides. Previous results indicated that the NTC complex is required for catalytic activation of the spliceosome and is recruited after U4 release. Our data indicate that the NTC is already integrated into the spliceosome at the B complex stage. Thus, earlier immunoprecipitation studies showing that the NTC is recruited concomitant to U4 snRNA release may be explained by a differential accessibility of the tag used for precipitation of B versus B^{act} (Chan et al., 2003). However, the NTC is clearly underrepresented in complex B as compared to later complexes (B^{act} and C). The majority of the human NTC proteins that have a yeast counterpart are also already found in the human B complex (Deckert et al., 2006). In addition to the NTC, two splicing factors that interact with components of the NTC and whose function is related to NTC in human and yeast (see below), namely Prp45 and Prp46 (human PRL1 and SKIP) (Albers et al., 2003), were also detected in complex B, suggesting that they potentially play a role in the transition from B to B^{act}.

The RNA helicase Prp5, an early splicing factor needed for the formation of the prespliceosome and the stable binding of U2 snRNP to the branch site (Ruby et al., 1993), was also found. Another factor detected in complex B is Urn1, which is homologous to human CA150, found in human A and B complexes (Behzadnia et al., 2007; Deckert et al., 2006). In conclusion, the total number of true spliceosomal factors associated with purified complex B is ~60, excluding the miscellaneous proteins related to RNA processing (listed in Supplemental Results).

A comparison of the proteome of B^{act} with that of B shows substantial differences. Proteins that were abundant in B, but not found in B^{act} or represented by only a few peptides, include all U1- and U4/U6-specific proteins (Table 1). All of the U6 snRNA-associated Lsm2–8 proteins were absent, consistent with the results of early studies that showed destabilization of these proteins during the activation of the spliceosome (Chan et al., 2003). The U5 proteins Prp6 and Dib1, all proteins specific for the tri-snRNP, plus Prp5 and Urn1 are likewise present in B, but not in B^{act}. Although immunoprecipitation data suggested that GST-Prp5 is associated with the spliceosome throughout the splicing cycle, the presence of a GST tag may have stabilized Prp5 association (Kosowski et al., 2009). In conclusion, ~35 proteins, more than half of the ~60 proteins found in complex B, are released or destabilized and then lost during purification.

Proteins recruited to B^{act} (i.e., not present in B) included ~12 proteins, several of which are well-established splicing factors or were previously detected in the endogenous Cef1-associated complex (Ohi et al., 2002). Among these are the NTC-related proteins, which are homologous to human proteins that either physically interact with Prp19 or CDC5L in humans or are

Table 1. Protein Composition of *S. cerevisiae* Spliceosomal Complexes B, B^{act}, and C

			Number of Peptides Sequenced in B, B^{act}, and C Complex Preparations								
Yeast Protein Name	Systematic Gene Name	MW (kDa)	M3-Actin Δ6		M3-Actin Δ6		M3-Actin Δ31	M3-Actin ACAC	Penta-snRNP	Cef1 TAP	Human Protein Name
			B #1	B #2	B^{act} #1	B^{act} #2	C #1	C #2			
pmol			2.0	0.5	1.5	0.5	0.8	0.8			
Sm Proteins											
B	YER029C	22.4	31	3	49	8	9	33	14	5	B
D1	YGR074W	16.3	22	4	3	5	5	10	8	1	D1
D2	YLR275W	12.8	26	9	27	7	10	6	5	3	D2
D3	YLR147C	11.2	14	4	3	10	6	8	5	2	D3
E	YOR159C	10.4	2	1	6	5	7	1	1		E
F	YPR182W	9.6	20	2	9	4	4	1	2	2	F
G	YFL017W-A	8.5	3	2	4	1	1	1	2	2	G
U1 snRNP Proteins											
Prp39	YML046W	74.7	27	8		1			3		
Snu71	YGR013W	71.4	26	8	1	1			3		S164
Prp40	YKL012W	69	19	12	1	4			7		FBP11
Prp42	YDR235W	65	17	7					2		
Nam8	YHR086W	56.9	5	3	1	3			2		TIA1/TIAR
Snu56	YDR240C	56.5	6	2					4		
Snp1	YIL061C	34.4	18	1					5		U1-70K
Mud1	YBR119W	34.4	14	5	1			1	3		U1-A
Luc7	YDL087C	30	1		2				2		LUC7B1
Yhc1	YLR298C	27	5						2		U1-C
U2 snRNP Proteins											
Rse1	YML049C	153.8	91	63	111	61	32	52	6	1	SF3b130
Hsh155	YMR288W	110	93	24	83	23	22	16	9	1	SF3b155
Prp9	YDL030W	63	70	25	66	45	14	12	7	2	SF3a60
Cus1	YMR240C	50.2	42	10	71	17	4	8	3		SF3b145
Prp21	YJL203W	33	50	4	35	16	5	14	13	2	SF3a120
Prp11	YDL043C	29.9	30	5	25	22	2	9	11	1	SF3a66
Lea1	YPL213W	27.2	28	3	47	11	22	17	10	6	U2-A′
Hsh49	YOR319W	24.5	4	2	41	2	6	2	9		SF3b49
Msl1	YIR009W	12.8	8		10	4	2	7	7	2	U2-B″
Rds3	YPR094W	12.3	3		4	1					SF3b14b
Ysf3	YNL138W-A	10	3	1	9	2	1	1			SF3b10
U5 snRNP Proteins											
Prp8	YHR165C	279.5	233	81	166	125	176	306	22	38	220K
Brr2	YER172C	246.2	197	90	237	197	110	126	30	17	200K
Snu114	YKL173W	114	66	54	159	51	113	130	18	24	116K
Prp6	YBR055C	104.2	73	37		1	4	11	29		102K
Prp28	YDR243C	66.6									100K
Lin1	YHR156C	40.4									52K
Dib1	YPR082C	16.7	10	1					5		15K
U4/U6 snRNP Proteins											
Prp31	YGR091W	56.3	27	11					12		61K
Prp3	YDR473C	56	27	11					29		90K
Prp4	YPR178W	52.4	27	14		1		2	12		60K
Snu13	YEL026W	13.6	2						3		15.5K

Table 1. *Continued*

Yeast Protein Name	Systematic Gene Name	MW (kDa)	Number of Peptides Sequenced in B, B^{act}, and C Complex Preparations								Human Protein Name
			M3-Actin Δ6		M3-Actin Δ6		M3-Actin Δ31	M3-Actin ACAC	Penta-snRNP	Cef1 TAP	
U4/U6.U5 snRNP Proteins											
Snu66	YOR308C	66.4	39	14					15		110K
Sad1	YFR005C	52.2							5		65K
Spp381	YBR152W	34	26	6					3		
Prp38	YGR075C	28	21	8	1	1	2	3	7		hPRP38
Snu23	YDL098C	23	33	8					13		hSNU23/ ZMAT2
Lsm Proteins											
LSm4	YER112W	21.3	16	3		1			5		LSm4
LSm7	YNL147W	13	3	1					2		LSm7
LSm8	YJR022W	12.4	3	1					4		LSm8
LSm2	YBL026W	11.2	8	4			2		2		LSm2
LSm5	YER146W	10.4	2	1							LSm5
LSm3	YLR438C	10	1						2		LSm3
LSm6	YDR378C	9.4	5	1	1				2		LSm6
RES Complex											
Bud13	YGL174W	30.5	23	4	81	26	11	30		1	MGC13125
Pml1	YLR016C	23.6	6		14	5	1	3	5		SNIP1 ?[a]
Ist/Snu17	YIR005W	17	3		12	2	3	1	7	1	CGI-79 ?[a]
NTC/Prp19 Complex											
Syf1	YDR416W	100	28	19	124	67	52	69	8	18	hSYF1/XAB2
Clf1	YLR117C	82.4	16	6	40	18	44	33	12	16	CRNKL1
Cef1	YMR213W	68	21	18	87	24	72	69	7	11	CDC5L
Prp19	YLL036C	56.6	49	31	235	50	195	150	13	17	hPRP19
Isy1	YJR050W	28	8	1	37	11	14	17	8	2	KIAA1160
Syf2	YGR129W	25	11	2	43	16	14	37	2	2	GCIP p29
Snt309	YPR101W	21	2	1	21	11	17	10	6	9	SPF27
Ntc20	YBR188C	16	11	2	8	1	2	11	3	4	
NTC-Related Proteins											
Prp46	YPL151C	51	20	9	97	35	20	28	7	20	PRL1
Prp45	YAL032C	42.5	19	5	70	15	13	37	18	16	SKIP1
Ecm2	YBR065C	41			35	5	26	32	1	8	RBM22 ?
Cwc2	YDL209C	38.4			43	19	9	45	11	5	RBM22
Cwc15	YDR163W	20			38	10	16	22		3	AD-002/ HSPC148
Bud31	YCR063W	18.4			12	1	4	11	10	2	G10
Early Splicing Factors											
Prp5[b]	YBR237W	96.4	10	5							hPRP5
Urn1[b]	YPR152C	54	8	5							TCERG1[d]
Known Splicing Factors											
Prp2	YNR011C	100			116	64	24	19			DDX16
Spp2	YOR148C	20.6			15	6	1	1			GPKOW/T54
Yju2	YKL095W	32			27	8	10	16		5	CCDC130
Cwc21	YDR482C	15.7			14	8	5	6		2	Srm300
Cwc22	YGR278W	67.3			48	17	33	67		2	KIAA1604
Cwc24	YLR323C	28			40	20	2	9			RNF113A

(*Continued on next page*)

Table 1. *Continued*

Yeast Protein Name	Systematic Gene Name	MW (kDa)	Number of Peptides Sequenced in B, B^{act}, and C Complex Preparations: M3-Actin Δ6	M3-Actin Δ6		M3-Actin Δ31	M3-Actin ACAC	Penta-snRNP	Cef1 TAP	Human Protein Name
Cwc27	YPL064C	35		29	11	2	6		1	NY-CO-10
Cwc23	YGL128C	33.2				2	3		2	DNAJ A1 ?[c]
Cwc25	YNL245C	20.4				2	3		1	CCDC49
Step 2 Proteins										
Prp17	YDR364C	52		24	10	14	36		5	hPRP17
Prp22	YER013W	130				24	68		2	hPRP22
Prp16	YKR086W	121.6					1			hPRP16
Slu7	YDR088C	44.6				2	17		1	hSLU7
Prp18	YGR006W	28.4				7	12			hPRP18
Disassembly Proteins[b]										
Prp43	YGL120C	87.6				9	2			hPRP43
Spp382	YLR424W	83				2	4			TFIP11
Ntr2	YKR022C	36.6				2				
CBP Proteins										
Sto1	YMR125W	100	7							CBP80[d]
Cbc2	YPL178W	24	1			1				CBP20[d]

Proteins were identified by LC-MSMS after separation by PAGE. Proteins identified in two out of two preparations are shown. Numbers represent the absolute number of peptides sequenced for a protein found in a particular preparation (i.e., #1 or #2). The table contains information about the *S. cerevisiae* protein, the systematic gene name, the calculated molecular weight in kDa, and the concentration in pmols of each complex analyzed by MS. Data from previous proteomic studies of purified endogenous penta-snRNP and Cef1-associated complex are also included (Ohi et al., 2002; Stevens et al., 2002). The last column contains the name of the human protein to aid comparison with previous studies of human spliceosomal complexes. Proteins are grouped in organizational and/or functional subgroups. Prp28, Lin1, and Sad1 were not detected by MS and are included for completeness.

[a] Homologs could not be assigned unambiguously on the basis of BLAST data.

[b] Never detected in yeast spliceosomal complexes.

[c] Extensive homology between protein family members prevents assignment of *S. cerevisiae* homologs on the basis of BLAST data.

[d] Human homolog previously detected in one or more human spliceosomal complex.

present with Prp19 in the human 35S U5 snRNP. Two of these proteins are also part of the human Prp19/CDC5L complex—Cwc15/AD002 and Prp46/PRL1—and are already integrated into human B complex (Deckert et al., 2006). Two additional members of the group—Bud31 and Ecm2—are homologous to the human Prp19-related proteins G10 and RBM22, respectively (Makarova et al., 2004).

A significant number of peptides were sequenced for the RNA helicase Prp2 and its binding partner Spp2, both of which are required prior to step 1. Thus, both of them are recruited during B^{act} formation, and their abundance is consistent with B^{act} being precatalytic. Yju2, which is also needed for step 1 and is known to promote step 1 after Prp2 function, is also found in B^{act} (Liu et al., 2007).

Surprisingly, of the step 2 splicing factors, Prp17 is present in abundance, whereas the other members of this group are absent. The recruitment of Prp17 to B^{act} is consistent with recent observations that Prp17 plays a role in step 1 (Sapra et al., 2008). In contrast, several well-established spliceosomal proteins known to act during step 2 of splicing were not found in B^{act}, as, for example, Prp22, Prp16, Slu7, and Prp18, suggesting that B^{act} is very pure. Indeed, this group of proteins is recruited at a later stage. In summary, the transition from the precatalytic B to the activated B^{act} complex involves a dramatic change in composition, in which more than 30 proteins dissociate from the spliceosome, and 12 new ones associate. Thus, B^{act} is composed of ~40 proteins.

Complex C formed on M3-ActΔ31 or M3-ActACAC has essentially the same protein composition (Table 1). Comparison of the proteomes of B^{act} and C reveals that all proteins of B^{act} are also contained in C. However, when the numbers of peptides of individual proteins are compared, it becomes clear that Prp2 and Spp2 are reproducibly less abundant in C. This suggests that their association is weakened during the transition from B^{act} to C, consistent with previous findings that Prp2 dissociates from the spliceosome concomitant with step 1 (Kim and Lin, 1996). Interestingly, this is also true for some components of the U2-associated, heteromeric SF3a complex and, in part, also SF3b. In contrast, the U5 proteins are present in equal abundance in B^{act} and C. Moreover, the numbers of peptides sequenced for proteins of the NTC and NTC-related complexes are generally higher in C than in B^{act}, indicating that these proteins are more stably bound and, thus, more abundant in the former.

A set of nine proteins that are not found in B and B^{act} were detected exclusively in C, implying that they are incorporated/stabilized into the spliceosome immediately before or during step 1. The most prominent of these are the step 2 factors Prp22, Slu7, and Prp18. Regarding the other two step 2 factors, Prp17 was already present in B^{act}, whereas Prp16 was only detected by one peptide. In fact, Prp16 appears to be only transiently associated with the spliceosome. Thus, complex C might be stalled at a stage after Prp16 has acted. It is also possible that the stalled C complex preparation contains both intermediate and second catalytic step conformations in addition to an off-pathway discard intermediate.

Two proteins recruited to the C complex are Cwc23 and Cwc25, both essential for growth but whose precise function is unknown (Ohi et al., 2002). The helicase Prp43 together with Spp382/Ntr1 and Ntr2 are also found in complex C (Table 1). This is in line with earlier observations that Spp382 and Ntr2 associate with Prp43 (forming the NTR complex) and thereby modulate its helicase activity (Tsai et al., 2007). The NTR complex is thus recruited to the spliceosome before step 2, even though it carries out its task later during the disassembly of the postspliceosomal complex (Tanaka et al., 2007). In summary, the biochemical composition of the spliceosome changes not only during early assembly steps, but also during the transition from B^{act} to C, although this compositional change is not as dramatic as that during the transition from B to B^{act}.

Electron Microscopy of Yeast Spliceosomes

To gain insights into the structure of yeast spliceosomes, we loaded purified complexes onto a glycerol gradient containing glutaraldehyde to fix the particles (Kastner et al., 2008). Particles from the peak fractions were negatively stained and analyzed by EM. To obtain a better resolution, we classified the single-particle images and averaged the members of each class. Results are summarized in Figure 4, which shows for each particle a typical EM field (left), a gallery of class averages (middle), and interpretative sketches (right). All three complexes showed monodisperse distributions with a particle size of ~40 nm.

Complex B exhibits in most projection classes a triangular or rhombic shape (Figure 4, uppermost block). The most conspicuous structural feature of the predominant classes (columns 1 and 2) is an almost straight element, ~30 Å long and 7–10 Å wide; in the orientation shown, this element runs from the bottom of the image (foot) to the upper left (stump). Classes looking approximately like mirror images of the main form are also found but rarely (column 3). Other more frequently seen forms include those shown in columns 4–6. These forms could be attributed to side-on views of complex B.

Complex B^{act} yielded images that were clearly different than those of B. Most classes show a protruding domain resembling that of the foot of complex B (shown pointing downward in the representations of B^{act}) (Figure 4). However, the main body appears more compact. The most frequent images of B^{act} (middle block, columns 1 and 2) display a slightly asymmetrical main body with outlines running left and right at different angles, such that the left appears steeper than the right. A more elongated accumulation of stain is found parallel to the left flank, whereas on the right, there is a point-like accumulation of stain. B^{act} also shows relatively frequent symmetric (column 3) and asymmetric (column 4) variants of the main form. Further typical images of B^{act} are shown in columns 5 and 6. On the left side, these show a pronounced axis, whereas the right side appears as a wing (column 6).

Complex C formed on M3-ActACAC also exhibits, in most image classes, an approximately straight element (Figure 4, lowest block). Here, however, the axis is always on the right side of the particle in the "foot-down" orientation (columns 1–4). Less-frequent forms include those shown in columns 5 and 6. In summary, the image classes of complex C appear less compact than those of B^{act}. Thus, the analysis of the EM images of the three purified complexes reveals structures of about the same size but with quite different morphology. The most pronounced structural differences are seen between B and B^{act}. Complex B^{act} and C also exhibit differences, but some views possess similar main features.

DISCUSSION

We have isolated in vitro assembled yeast spliceosomal complexes under low-stringency conditions. A comparison of their protein compositions revealed a drastic exchange of proteins during the transition from B to B^{act}. During the B^{act}-to-C transition, the spliceosome is also significantly remodeled. Prp2/Spp2 are destabilized, and U2 SF3a/b proteins are underrepresented, suggesting that they are less stably associated and lost during purification of complex C. EM revealed that these compositional dynamics correlate with structural changes during both transitions (e.g., B to B^{act} and B^{act} to C).

Yeast Spliceosomes Have Radically Fewer Proteins Than Do Metazoans

The human and *Drosophila* B complexes isolated under similar mild conditions contain ~110 proteins (Deckert et al., 2006; Herold et al., 2009), whereas the yeast B complex comprises ~60 proteins. Differences between the C complex from different organisms are even more significant, with ~110 proteins in metazoans versus ~50 in yeast. Thus, the number of proteins per spliceosomal complex is less than half (Figure 5). We identified, altogether, ~90 proteins in the three complexes that we purified and characterized here (Table 1 and Figure 5), excluding the group of miscellaneous proteins related to RNA processing, as their role in splicing has not clearly been demonstrated so far (Table S1). Proteins identified here also include the majority of those previously found in the purified penta-snRNP and in the endogenous Cef1-associated complex (Ohi et al., 2002; Stevens et al., 2002). Established splicing factors that were discovered by genetics or other techniques, which were not found in our spliceosomal complexes, include those that are either loosely associated and lost during purification, such as Prp28 and Sad1, or those that act earlier during spliceosome assembly, e.g., Mud2, Msl5, and Npl3. It is possible that some additional factors will be discovered. Nevertheless, the total number of yeast spliceosomal proteins will likely be less than 100. In contrast, the total number of proteins thus far identified in metazoan spliceosomal complexes lies in the range of 170 (human)

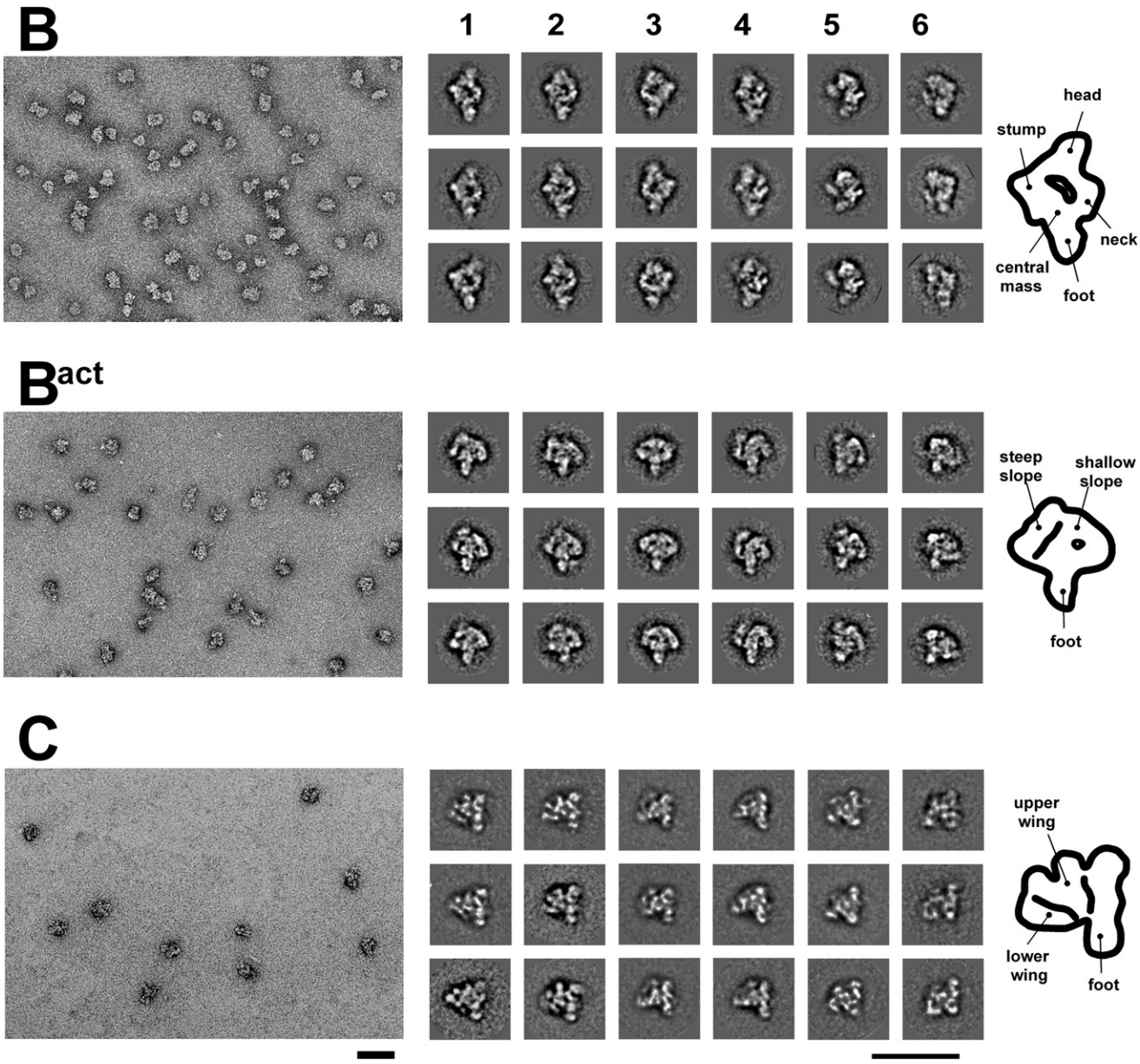

Figure 4. Electron Microscopy of Yeast Spliceosomes

Overviews of negatively stained samples are shown in the left panels. Representative class averages are shown in the galleries in the middle (numbered 1 to 6), starting with the most frequently observed class, for which a schematic drawing is shown on the right. All three particles display a short protuberance that in the class averages is shown pointing downward (foot). Some structural features are labeled. Names introduced by Boehringer et al. (2004) for the human B complex are used also for the yeast B complex. A small fraction of images typical of the most frequent classes of complex B^{act} was also detected in the C complex preparation. Scale bars, 50 nm.

(Figure 5) and 190 (*Drosophila*), counting only proteins identified in spliceosomes isolated under native conditions by two-step purifications and excluding more specialized tissue-specific splicing regulatory proteins.

Evolutionary Conservation of Yeast Spliceosomes

Although the number of splicing factors found associated with purified human spliceosomes is much larger than those found in yeast spliceosomes, nearly all of the identified yeast splicing factors are evolutionarily conserved in humans. Strikingly, more than 85% of the yeast splicing factors listed in Table 1 have a clear evolutionarily conserved counterpart (Figure 5). Only a handful of proteins do not have an obvious human counterpart. Thus, the yeast splicing machinery likely represents the evolutionarily conserved core design of the spliceosome.

Figure 5 also shows that ~80 human proteins that associate with purified spliceosomal complexes do not have an obvious conserved counterpart in yeast (shown below the rectangle).

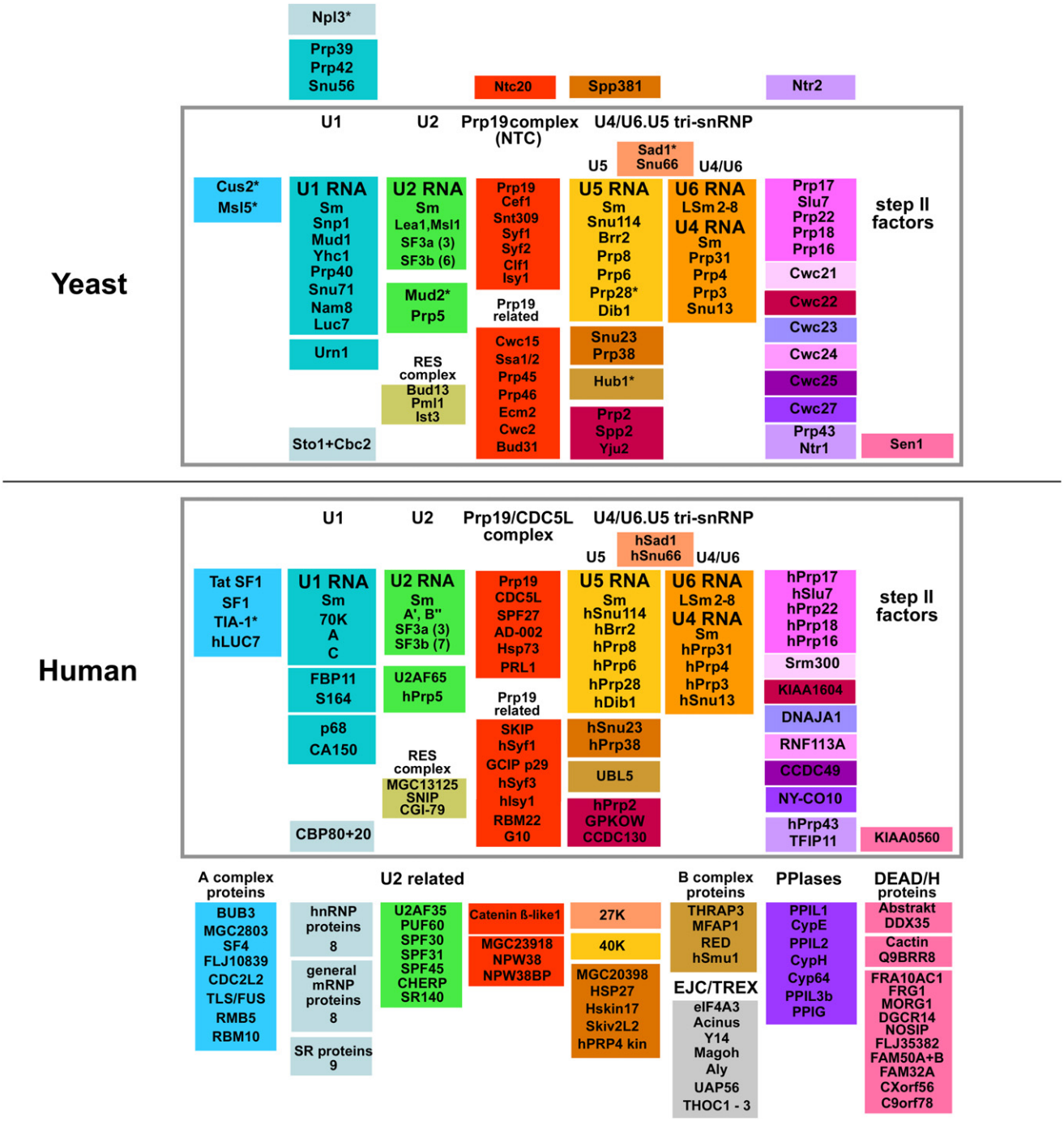

Figure 5. The Yeast Splicing Machinery Is Less Complex Than that of Humans

(Yeast) Proteins (yeast nomenclature) evolutionarily conserved between yeast and man, associated with purified yeast B, B^{act}, and C complexes, are placed inside of the rectangle. Proteins above the rectangle do not have a human counterpart. (Human) Proteins (human nomenclature) evolutionarily conserved between yeast and man, associated with purified human A, B, and C complexes, are placed inside of the rectangle. Proteins below the rectangle were found associated with purified human spliceosomal complexes, but the majority of them do not have a yeast counterpart (Behzadnia et al., 2007; Bessonov et al., 2008). Numbers indicate the total number of individual proteins in a particular group. (Asterisks) Proteins that do have homologs in yeast or human but were not found or found loosely associated with purified spliceosomal complexes; yeast Msl5, Npl3, Mud2, and Hub1 were found with low peptide numbers in the 20S–25S peak described above for the B complex. Cus2, Prp28, and Sad1 were not detected by MS and are included for completeness, as well as human TIA-1, which is the homolog of yeast Nam8. Proteins are grouped according to snRNP association, function, presence in a stable heteromeric complex, or association with a particular spliceosomal complex, as indicated.

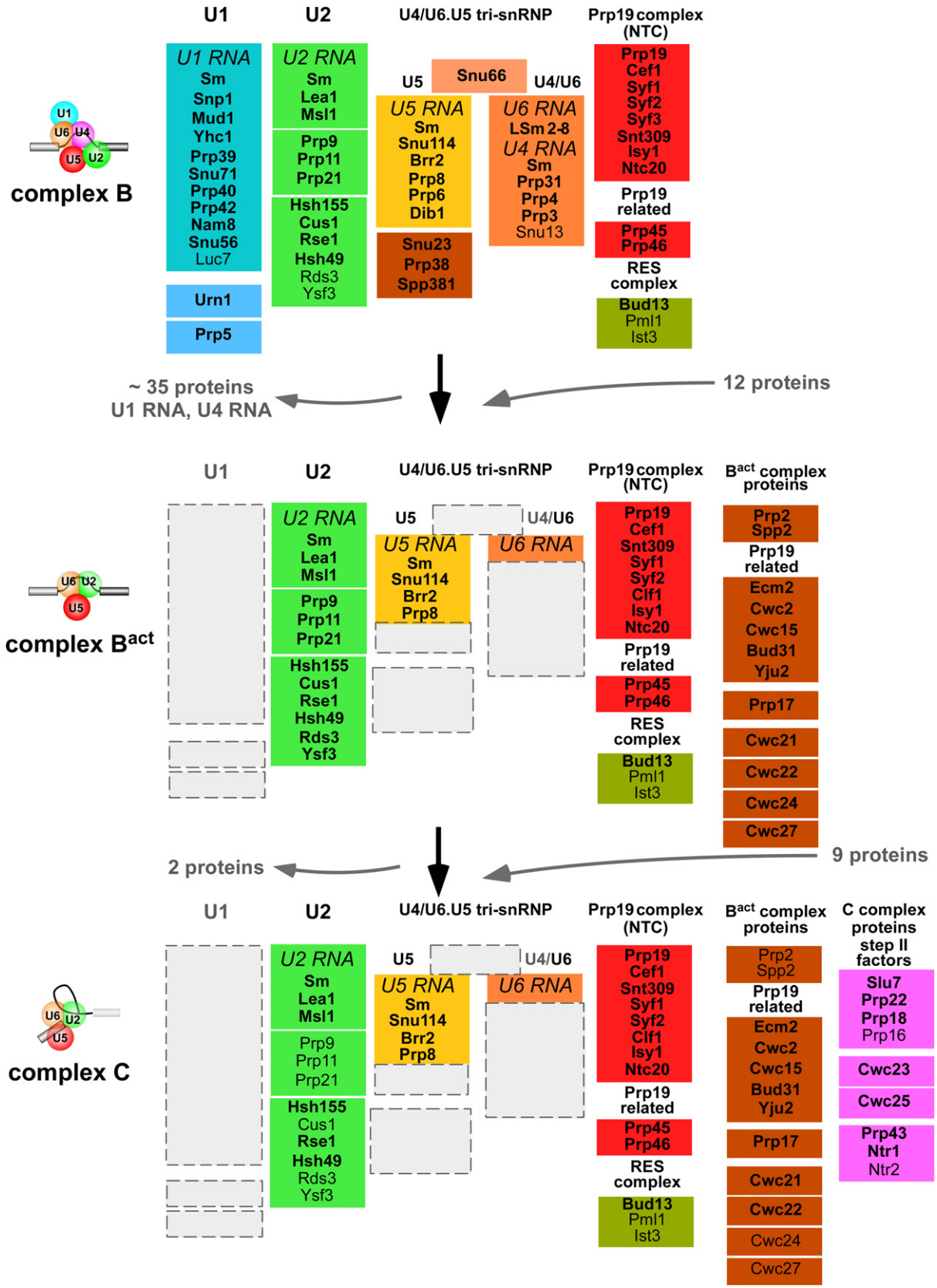
U1
U2
U4/U6.U5 tri-snRNP
Prp19 complex (NTC)
U1 RNA
Sm
Snp1
Mud1
Yhc1
Prp39
Snu71
Prp40
Prp42
Nam8
Snu56
Luc7
Urn1
Prp5
U2 RNA
Sm
Lea1
Msl1
Prp9
Prp11
Prp21
Hsh155
Cus1
Rse1
Hsh49
Rds3
Ysf3
U5
Snu66
U4/U6
U5 RNA
Sm
Snu114
Brr2
Prp8
Prp6
Dib1
Snu23
Prp38
Spp381
U6 RNA
LSm 2-8
U4 RNA
Sm
Prp31
Prp4
Prp3
Snu13
Prp19
Cef1
Syf1
Syf2
Syf3
Snt309
Isy1
Ntc20
Prp19 related
Prp45
Prp46
RES complex
Bud13
Pml1
Ist3
complex B
~ 35 proteins
U1 RNA, U4 RNA
12 proteins
U1
U2
U4/U6.U5 tri-snRNP
Prp19 complex (NTC)
Bact complex proteins
U2 RNA
Sm
Lea1
Msl1
Prp9
Prp11
Prp21
Hsh155
Cus1
Rse1
Hsh49
Rds3
Ysf3
U5
U4/U6
U5 RNA
Sm
Snu114
Brr2
Prp8
U6 RNA
Prp19
Cef1
Snt309
Syf1
Syf2
Clf1
Isy1
Ntc20
Prp19 related
Prp45
Prp46
RES complex
Bud13
Pml1
Ist3
Prp2
Spp2
Prp19 related
Ecm2
Cwc2
Cwc15
Bud31
Yju2
Prp17
Cwc21
Cwc22
Cwc24
Cwc27
complex Bact
2 proteins
9 proteins
U1
U2
U4/U6.U5 tri-snRNP
Prp19 complex (NTC)
Bact complex proteins
C complex proteins step II factors
U2 RNA
Sm
Lea1
Msl1
Prp9
Prp11
Prp21
Hsh155
Cus1
Rse1
Hsh49
Rds3
Ysf3
U5
U4/U6
U5 RNA
Sm
Snu114
Brr2
Prp8
U6 RNA
Prp19
Cef1
Snt309
Syf1
Syf2
Clf1
Isy1
Ntc20
Prp19 related
Prp45
Prp46
RES complex
Bud13
Pml1
Ist3
Prp2
Spp2
Prp19 related
Ecm2
Cwc2
Cwc15
Bud31
Yju2
Prp17
Cwc21
Cwc22
Cwc24
Cwc27
Slu7
Prp22
Prp18
Prp16
Cwc23
Cwc25
Prp43
Ntr1
Ntr2
complex C

These include, among others, SR and hnRNP proteins, which are known to play a role in regulating alternative splicing (Wahl et al., 2009). A set of about ten SR and hnRNP proteins and several U2-related proteins are present in early human spliceosomes but essentially absent from yeast (Figure 5). Thus, we may expect that one or more yeast SR-like or hnRNP protein will be found in early yeast spliceosomal complexes (e.g., complex A). Indeed, although yeast does not possess canonical SR proteins, the SR-like protein Npl3 was recently shown to promote the recruitment of the U1 snRNP to the pre-mRNA (Kress et al., 2008).

In order to splice a wide variety of pre-mRNAs, the human spliceosome contains many regulatory proteins that are loosely associated and only required in certain situations. Obvious counterparts for many of these proteins are not present in yeast. For example, at least seven proteins of the PPIase family (peptidyl-prolyl *cis/trans* isomerases) are found in human spliceosomes (Figure 5). Only one PPIase, NY-CO-10, shows 28% identity (45% similarity) with yeast Cwc27, which harbors a PPIase domain. This indicates that the yeast splicing machinery is less complex than that of metazoans due to the limited amount of regulated splicing.

Spliceosomal Dynamics in Yeast during Catalytic Activation

Comparative proteomics of human and *Drosophila* spliceosomal B and C complexes revealed that more than 60 proteins are exchanged during catalytic activation of the metazoan splicing machinery (Bessonov et al., 2008; Herold et al., 2009). Here, we show that the compositional dynamics of the splicing machinery during catalytic activation is evolutionarily conserved between yeast and metazoans. Moreover, the dissociation and recruitment of proteins appears to occur in discrete steps. The most dramatic compositional change occurs during the transition from the precatalytic yeast B to the activated B^{act} complex. During this transition, the entire U1 snRNP is released, whereas the tri-snRNP undergoes massive remodeling. This entails dramatic structural rearrangements that at the RNA level involve unwinding of the U4/U6 base-pairing interaction and the formation of U2/U6 base pairing, a reorganization that is unprecedented among RNP machines (Wahl et al., 2009).

Concomitant with U4/U6 unwinding, the U4 snRNA and all U4/U6-associated proteins are released from the spliceosome together with proteins that tether the U5 to the U4/U6 snRNP (Figure 6) (Häcker et al., 2008). Consistent with this, B^{act} lacks all U4/U6 proteins and several U5-specific proteins (Figure 6). Furthermore, as indicated by previous studies, the Lsm proteins dissociate at the time of spliceosome activation (Chan et al., 2003). As the U6 snRNA has been liberated from several precatalytic binding partners, new partners must be provided to stabilize U6 interaction with the pre-mRNA and the U2 snRNA. The number and nature of proteins promoting formation of the U2/U6 base-pairing interaction is unclear, as well as the precise time at which such proteins are recruited. Components of the NTC complex and/or NTC-related proteins play an important role in this process, as shown previously (Chan et al., 2003) and discussed below.

We show that 12 known splicing factors are clearly recruited at the time of activation (Figure 6, B^{act} proteins). Thus, we consider these proteins a hallmark of the activated B^{act} complex. At least two classes of proteins belong to this group: (1) those most probably required to establish and/or stabilize the U2/U6 base-pairing interaction (e.g., Ecm2 and, most probably, Cwc2, a protein that contains an RNA recognition motif [RRM]; McGrail et al., 2009) and (2) those more directly required to promote step 1, such as Prp2, Spp2, and Yju2. The presence of the splicing factor Ecm2 in B^{act} is consistent with its function in promoting the annealing of the U2/U6 helix II (Xu and Friesen, 2001).

Prp2 is the only RNA helicase known to act subsequently to U4/U6 unwinding by Brr2 but prior to step 1. Although the exact role of Prp2 is not well understood, it may control another rearrangement that leads from a formally activated spliceosome (characterized by the removal of U1 and U4) to a particle that is catalytically competent for step 1 (Kim and Lin, 1996). It was suggested that Prp2 leaves the spliceosome following ATP hydrolysis. However, we show that it remains stably bound in B^{act}, suggesting that Prp2 in this particular spliceosomal configuration cannot hydrolize ATP; otherwise, it would dissociate. We thus conclude that B^{act} is not yet catalytically activated. This is further confirmed by the high S value of B^{act} (45S) and is consistent with previous studies that showed that, prior to ATP hydrolysis, the spliceosome has a higher S value than it has after ATP hydrolysis (Kim and Lin, 1996). Our finding that Prp2 is "trapped" in B^{act} provides a biochemical explanation as to why spliceosomes assembled on M3-ActΔ6 pre-mRNA at high ATP concentrations undergo activation but do not proceed to step 1 catalysis. It is tempting to speculate that a longer RNA stretch downstream of the branch site may be required—either directly or as a protein-binding site—to stimulate ATP hydrolysis and/or to support the structural rearrangement of the spliceosome that occurs during Prp2-mediated ATP hydrolysis and release. Thus, B^{act} very likely represents a spliceosome prior to the final catalytic activation step mediated by Prp2. Therefore, we cannot exclude that one or more proteins present in the purified complex C may, in fact, be required for promoting step 1.

Yju2 is also recruited at the time of activation and, like Prp2, acts in concert with an unidentified HP factor(s) to promote step 1 after the Prp2-mediated structural rearrangement of the spliceosome (Liu et al., 2007). B^{act}, however, contains stably bound Prp2. Thus, Yju2 is recruited prior to Prp2 action in B^{act}, most likely to support the rearrangements organized by Prp2 and/or to provide a recruitment platform for one or more additional proteins required for promoting step 1.

Comparison of B^{act} and C shows that the conversion from an activated to a catalytic step 1 spliceosome also entails major

Figure 6. Compositional Dynamics of Yeast Spliceosomes

The protein composition of the yeast B, B^{act}, and C complexes was determined by MS. Proteins (yeast nomenclature) are grouped as described in the legend of Figure 5. The relative abundance of proteins is indicated by light (substoichiometric amounts) or dark (stoichiometric amounts) lettering and is based on the relative number of peptides sequenced (Table 1) (Supplemental Experimental Procedures).

remodeling. Following Prp2 action, Prp2/Spp2 are both destabilized, as determined by the decrease in the number of peptides sequenced by MS (Table 1). The reduction in Prp2/Spp2 is accompanied by a lower S value of complex C (40S) and by a decrease in proteins comprising the U2-associated SF3a and, in part, SF3b complexes. In yeast, step 2 of splicing can proceed in the absence of U2/branch site sequence base pairing (Smith et al., 2007). Thus, whereas SF3a/b are essential early in the splicing reaction, they may not be required after step 1.

Interestingly, key proteins that function at later stages of the splicing reaction are recruited to complex C. At least nine proteins are recruited during C complex formation and step 1 of splicing. These include most step 2 factors (Umen and Guthrie, 1995) (Figure 6), suggesting that they function within a multicomponent complex and, with the exception of Prp17, which can be considered a bona fide step 1 factor, are recruited together during/after step 1. Also, the trimeric disassembly NTR complex is already recruited to complex C. Although the NTR complex may facilitate RNP conformational changes accompanying release of splicing intermediates, it is recruited during or immediately after step 1, even if step 2 and exon ligation cannot take place, as the pre-mRNA is mutated and/or missing the 3′ss. Alternatively, the unexpected association of the NTR with the C complex may suggest turnover of stalled spliceosomes (Pandit et al., 2006).

Cwc23 and Cwc25 are both recruited during C complex formation, and to date, no functions have been described for either of them. It will be interesting to investigate whether they are required for step 1 or later steps in the spliceosomal cycle. In conclusion, the proteins present in complex C likely comprise the complete list of proteins required to maintain a functional RNP machine in which step 1 occurs (Figure 6). As the complete set of known step 2 factors is present in complex C, this indicates that step 2 could also occur under certain conditions and on a wild-type pre-mRNA substrate. The limited number of proteins recruited during the B^{act}-to-C transition offers the exciting possibility of investigating step 1 and 2 in vitro using purified components of known composition.

Compositional Dynamics Correlate with Structural Changes

EM showed that the B, B^{act}, and C complexes exhibit distinct typical shapes (Figure 4). Complex B images have triangular/rhombic shapes that are very similar to corresponding images obtained for human and *Drosophila* B complexes (Deckert et al., 2006; Herold et al., 2009). In addition, structural features first described for the human complex (Boehringer et al., 2004), such as head, neck, stump, and foot, are also discernable in the yeast complex. This suggests that higher-order interactions and the general spatial organization of spliceosomal subunits are also conserved among metazoans and yeast. The most evident difference between B complexes from yeast and man lies in the size of the head region, which is substantially smaller in yeast. The structural heterogeneity observed for complex B's head domain in other organisms (Boehringer et al., 2004; Deckert et al., 2006) is also seen in the yeast complex, but here, the degree of heterogeneity is less pronounced. B and B^{act} are structurally the most distinct, in agreement with substantial differences in protein/RNA composition and the profound compositional remodeling during the B-to-B^{act} transition. Remodeling also leads to a change in sedimentation behavior—from 40 to 45S—during this activation step.

Our EM studies indicated that there are profound structural differences also between the 2D class averages of B^{act} and C. This is also reflected in the S value, which drops again to 40S for the less-compact appearing C complex. The observed structural differences could result from remodeling occurring concomitant with 5′ss cleavage in complex C. Thus, consistent with mechanistic differences between B^{act} and C, their 2D structures suggest differences in their spatial organization. EM immunolabeling of spliceosomal components and 3D reconstructions may allow a more precise determination of the structural differences between B^{act} and C spliceosomes.

EXPERIMENTAL PROCEDURES

Details of in vitro splicing, purification of spliceosomes, and mass spectrometric analyses are given in the Supplemental Experimental Procedures.

Purification of Yeast Spliceosomes

To isolate spliceosomal complexes under native conditions, before splicing we incubated M3-Act pre-mRNA wild-type or truncated forms with a 35-fold molar excess of purified MS2-MBP fusion protein at 4°C for 30 min in 20 mM HEPES-KOH (pH 7.9). To purify preparative amounts of complexes, a 36–72 ml splicing reaction containing 2–2.5 nM of [^{32}P]-labeled M3-Act pre-mRNA (specific activity 150–200 cpm/fmol) was performed in 60 mM K-PO_4 (pH 7.4), 3% PEG 8000, 2.5 mM $MgCl_2$, 2.0 mM ATP, 2.0 mM spermidine, and 40% yeast extract in buffer D (20 mM HEPES-KOH [pH 7.9], 50 mM KCl, 0.2 mM EDTA pH 8.0, 20% [v/v] glycerol, 0.5 mM DTT, and 0.5 mM PMSF). B and B^{act} were assembled by incubating at 23°C for 50 min; C complex, for 60 min (Supplemental Experimental Procedures).

Electron Microscopy

Eluted complexes were fixed by loading onto a 3.8 ml linear 10%–30% glycerol gradient containing 0.1% gluteraldehyde in the 30% gradient solution and centrifuged for 107 min at 490,000 g (Kastner et al., 2008). Gradients were fractionated from the bottom using a fraction collector. Particles were negatively stained by the double-carbon film method (Golas et al., 2003). Images were taken at 160 kV and a magnification of 88,000 or 115,000 in eucentric height at a defocus of ~1.5 μm in a CM200FEG microscope (FEI, Eindhoven, The Netherlands) at RT on a 4 k × 4 k CCD camera (TVIPS GmbH, Gauting, Germany) using 2-fold pixel binning. About 10,000 particle images were collected for each data set and were subjected to single-particle image processing at the level of 2D projection images using the IMAGIC-V software package (Image Science GmbH, Berlin, Germany). Good-quality class averages were obtained after several iterations of alignment, multivariate statistical analysis (MSA), and classification.

SUPPLEMENTAL DATA

Supplemental Data include Supplemental Results, Supplemental Experimental Procedures, four figures, and one table and can be found with this article online at http://www.cell.com/molecular-cell/supplemental/S1097-2765(09)00700-X.

ACKNOWLEDGMENTS

We thank M. Raabe and U. Plessmann for help with the MS analysis, R. Karaduman and N. Rasche for help with preparing MS2 substrates and proteins, R. Rauhut for help in homology searches, and C.L. Will for comments on the manuscript. This work was supported by grants from the European

Commission (EURASNET-518238) and the Ernst Jung Stiftung to R.L. and a YIP grant from EURASNET to H.U.

Received: May 15, 2009
Revised: July 14, 2009
Accepted: September 2, 2009
Published: November 25, 2009

REFERENCES

Abelson, J. (2008). Is the spliceosome a ribonucleoprotein enzyme? Nat. Struct. Mol. Biol. *15*, 1235–1237.

Albers, M., Diment, A., Muraru, M., Russell, C.S., and Beggs, J.D. (2003). Identification and characterization of Prp45p and Prp46p, essential pre-mRNA splicing factors. RNA *9*, 138–150.

Behzadnia, N., Golas, M.M., Hartmuth, K., Sander, B., Kastner, B., Deckert, J., Dube, P., Will, C.L., Urlaub, H., Stark, H., and Lührmann, R. (2007). Composition and three-dimensional EM structure of double affinity-purified, human prespliceosomal A complexes. EMBO J. *26*, 1737–1748.

Bessonov, S., Anokhina, M., Will, C.L., Urlaub, H., and Lührmann, R. (2008). Isolation of an active step I spliceosome and composition of its RNP core. Nature *452*, 846–850.

Boehringer, D., Makarov, E.M., Sander, B., Makarova, O.V., Kastner, B., Lührmann, R., and Stark, H. (2004). Three-dimensional structure of a pre-catalytic human spliceosomal complex B. Nat. Struct. Mol. Biol. *11*, 463–468.

Brow, D.A. (2002). Allosteric cascade of spliceosome activation. Annu. Rev. Genet. *36*, 333–360.

Caceres, J.F., and Kornblihtt, A.R. (2002). Alternative splicing: multiple control mechanisms and involvement in human disease. Trends Genet. *18*, 186–193.

Chan, S.P., Kao, D.I., Tsai, W.Y., and Cheng, S.C. (2003). The Prp19p-associated complex in spliceosome activation. Science *302*, 279–282.

Cheng, S.C. (1994). Formation of the yeast splicing complex A1 and association of the splicing factor PRP19 with the pre-mRNA are independent of the 3′ region of the intron. Nucleic Acids Res. *22*, 1548–1554.

Cheng, S.C., and Abelson, J. (1987). Spliceosome assembly in yeast. Genes Dev. *1*, 1014–1027.

Deckert, J., Hartmuth, K., Boehringer, D., Behzadnia, N., Will, C.L., Kastner, B., Stark, H., Urlaub, H., and Lührmann, R. (2006). Protein composition and electron microscopy structure of affinity-purified human spliceosomal B complexes isolated under physiological conditions. Mol. Cell. Biol. *26*, 5528–5543.

Dziembowski, A., Ventura, A.P., Rutz, B., Caspary, F., Faux, C., Halgand, F., Laprevote, O., and Seraphin, B. (2004). Proteomic analysis identifies a new complex required for nuclear pre-mRNA retention and splicing. EMBO J. *23*, 4847–4856.

Golas, M.M., Sander, B., Will, C.L., Lührmann, R., and Stark, H. (2003). Molecular architecture of the multiprotein splicing factor SF3b. Science *300*, 980–984.

Gottschalk, A., Neubauer, G., Banroques, J., Mann, M., Lührmann, R., and Fabrizio, P. (1999). Identification by mass spectrometry and functional analysis of novel proteins of the yeast [U4/U6.U5] tri-snRNP. EMBO J. *18*, 4535–4548.

Häcker, I., Sander, B., Golas, M.M., Wolf, E., Karagoz, E., Kastner, B., Stark, H., Fabrizio, P., and Lührmann, R. (2008). Localization of Prp8, Brr2, Snu114 and U4/U6 proteins in the yeast tri-snRNP by electron microscopy. Nat. Struct. Mol. Biol. *15*, 1206–1212.

Herold, N., Will, C.L., Wolf, E., Kastner, B., Urlaub, H., and Lührmann, R. (2009). Conservation of the protein composition and electron microscopy structure of Drosophila melanogaster and human spliceosomal complexes. Mol. Cell. Biol. *29*, 281–301.

Hertel, K.J., and Graveley, B.R. (2005). RS domains contact the pre-mRNA throughout spliceosome assembly. Trends Biochem. Sci. *30*, 115–118.

Jurica, M.S., and Moore, M.J. (2002). Capturing splicing complexes to study structure and mechanism. Methods *28*, 336–345.

Kastner, B., Fischer, N., Golas, M.M., Sander, B., Dube, P., Boehringer, D., Hartmuth, K., Deckert, J., Hauer, F., Wolf, E., et al. (2008). GraFix: sample preparation for single-particle electron cryomicroscopy. Nat. Methods *5*, 53–55.

Kim, S.H., and Lin, R.J. (1996). Spliceosome activation by PRP2 ATPase prior to the first transesterification reaction of pre-mRNA splicing. Mol. Cell. Biol. *16*, 6810–6819.

Kosowski, T.R., Keys, H.R., Quan, T.K., and Ruby, S.W. (2009). DExD/H-box Prp5 protein is in the spliceosome during most of the splicing cycle. RNA *15*, 1345–1362.

Kress, T.L., Krogan, N.J., and Guthrie, C. (2008). A single SR-like protein, Npl3, promotes pre-mRNA splicing in budding yeast. Mol. Cell *32*, 727–734.

Liu, Y.C., Chen, H.C., Wu, N.Y., and Cheng, S.C. (2007). A novel splicing factor, Yju2, is associated with NTC and acts after Prp2 in promoting the first catalytic reaction of pre-mRNA splicing. Mol. Cell. Biol. *27*, 5403–5413.

Makarova, O.V., Makarov, E.M., Urlaub, H., Will, C.L., Gentzel, M., Wilm, M., and Lührmann, R. (2004). A subset of human 35S U5 proteins, including Prp19, function prior to catalytic step 1 of splicing. EMBO J. *23*, 2381–2391.

McGrail, J.C., Krause, A., and O'Keefe, R.T. (2009). The RNA binding protein Cwc2 interacts directly with the U6 snRNA to link the nineteen complex to the spliceosome during pre-mRNA splicing. Nucleic Acids Res. *37*, 4205–4217.

Nilsen, T.W. (1998). RNA-RNA interactions in nuclear pre-mRNA splicing. In RNA Structure and Function, M. Grundber-Manago and R.W. Simons, eds. (Cold Spring Harbor, NY: Cold Spring Harbor Laboratory Press), pp. 279–307.

Ohi, M.D., Link, A.J., Ren, L., Jennings, J.L., McDonald, W.H., and Gould, K.L. (2002). Proteomics analysis reveals stable multiprotein complexes in both fission and budding yeasts containing Myb-related Cdc5p/Cef1p, novel pre-mRNA splicing factors, and snRNAs. Mol. Cell. Biol. *22*, 2011–2024.

Pandit, S., Lynn, B., and Rymond, B.C. (2006). Inhibition of a spliceosome turnover pathway suppresses splicing defects. Proc. Natl. Acad. Sci. USA *103*, 13700–13705.

Pyle, A.M. (2008). Translocation and unwinding mechanisms of RNA and DNA helicases. Annu. Rev. Biophys. *37*, 317–336.

Ruby, S.W., Chang, T.H., and Abelson, J. (1993). Four yeast spliceosomal proteins (PRP5, PRP9, PRP11, and PRP21) interact to promote U2 snRNP binding to pre-mRNA. Genes Dev. *7*, 1909–1925.

Rymond, B.C., and Rosbash, M. (1985). Cleavage of 5′ splice site and lariat formation are independent of 3′ splice site in yeast mRNA splicing. Nature *317*, 735–737.

Sapra, A.K., Khandelia, P., and Vijayraghavan, U. (2008). The splicing factor Prp17 interacts with the U2, U5 and U6 snRNPs and associates with the spliceosome pre- and post-catalysis. Biochem. J. *416*, 365–374.

Small, E.C., Leggett, S.R., Winans, A.A., and Staley, J.P. (2006). The EF-G-like GTPase Snu114p regulates spliceosome dynamics mediated by Brr2p, a DExD/H box ATPase. Mol. Cell *23*, 389–399.

Smith, D.J., Query, C.C., and Konarska, M.M. (2007). trans-splicing to spliceosomal U2 snRNA suggests disruption of branch site-U2 pairing during pre-mRNA splicing. Mol. Cell *26*, 883–890.

Stevens, S.W., and Abelson, J. (1999). Purification of the yeast U4/U6.U5 small nuclear ribonucleoprotein particle and identification of its proteins. Proc. Natl. Acad. Sci. USA *96*, 7226–7231.

Stevens, S.W., Ryan, D.E., Ge, H.Y., Moore, R.E., Young, M.K., Lee, T.D., and Abelson, J. (2002). Composition and functional characterization of the yeast spliceosomal penta-snRNP. Mol. Cell *9*, 31–44.

Tanaka, N., Aronova, A., and Schwer, B. (2007). Ntr1 activates the Prp43 helicase to trigger release of lariat-intron from the spliceosome. Genes Dev. *21*, 2312–2325.

Tarn, W.Y., Lee, K.R., and Cheng, S.C. (1993). Yeast precursor mRNA processing protein PRP19 associates with the spliceosome concomitant with or just after dissociation of U4 small nuclear RNA. Proc. Natl. Acad. Sci. USA *90*, 10821–10825.

Tsai, R.T., Tseng, C.K., Lee, P.J., Chen, H.C., Fu, R.H., Chang, K.J., Yeh, F.L., and Cheng, S.C. (2007). Dynamic interactions of Ntr1-Ntr2 with Prp43 and with U5 govern the recruitment of Prp43 to mediate spliceosome disassembly. Mol. Cell. Biol. *27*, 8027–8037.

Umen, J.G., and Guthrie, C. (1995). The second catalytic step of pre-mRNA splicing. RNA *1*, 869–885.

Vijayraghavan, U., Parker, R., Tamm, J., Iimura, Y., Rossi, J., Abelson, J., and Guthrie, C. (1986). Mutations in conserved intron sequences affect multiple steps in the yeast splicing pathway, particularly assembly of the spliceosome. EMBO J. *5*, 1683–1695.

Wahl, M.C., Will, C.L., and Lührmann, R. (2009). The spliceosome: Design principles of a dynamic RNP machine. Cell *136*, 701–718.

Xu, D., and Friesen, J.D. (2001). Splicing factor Slt11p and its involvement in formation of U2/U6 helix II in activation of the yeast spliceosome. Mol. Cell. Biol. *21*, 1011–1023.